

## Initial decomposition mechanism for the energy release from electronically excited energetic materials: FOX-7 (1,1-diamino-2,2-dinitroethene, $C_2H_4N_4O_4$ )

Bing Yuan, Zijun Yu, and Elliot R. Bernstein

Citation: *The Journal of Chemical Physics* **140**, 074708 (2014); doi: 10.1063/1.4865266

View online: <http://dx.doi.org/10.1063/1.4865266>

View Table of Contents: <http://aip.scitation.org/toc/jcp/140/7>

Published by the *American Institute of Physics*

---

### Articles you may be interested in

Initial mechanisms for the unimolecular decomposition of electronically excited nitrogen-rich energetic materials with tetrazole rings: 1-DTE, 5-DTE, BTA, and BTH

*The Journal of Chemical Physics* **144**, 234302234302 (2016); 10.1063/1.4953552

---

**COMPLETELY**

**REDESIGNED!**



**PHYSICS  
TODAY**

*Physics Today* Buyer's Guide  
Search with a purpose.

# Initial decomposition mechanism for the energy release from electronically excited energetic materials: FOX-7 (1,1-diamino-2,2-dinitroethene, $C_2H_4N_4O_4$ )

Bing Yuan, Zijun Yu, and Elliot R. Bernstein<sup>a)</sup>

*Department of Chemistry, Colorado State University, Fort Collins, Colorado 80523-1872, USA*

(Received 12 December 2013; accepted 28 January 2014; published online 19 February 2014)

Decomposition of the energetic material FOX-7 (1,1-diamino-2,2-dinitroethylene,  $C_2H_4N_4O_4$ ) is investigated both theoretically and experimentally. The NO molecule is observed as an initial decomposition product subsequent to electronic excitation. The observed NO product is rotationally cold ( $<35$  K) and vibrationally hot (2800 K). The initial decomposition mechanism is explored at the complete active space self-consistent field (CASSCF) level. Potential energy surface calculations at the CASSCF(12,8)/6-31G(d) level illustrate that conical intersections play an essential role in the decomposition mechanism. Electronically excited  $S_2$  FOX-7 can radiationlessly relax to lower electronic states through  $(S_2/S_1)_{CI}$  and  $(S_1/S_0)_{CI}$  conical intersections and undergo a nitro-nitrite isomerization to generate NO product on the  $S_0$  state. The theoretically predicted mechanism is consistent with the experimental results. As FOX-7 decomposes on the ground electronic state, thus, the vibrational energy of the NO product from FOX-7 is high. The observed rotational energy distribution for NO is consistent with the final transition state structure on the  $S_0$  state. Ground state FOX-7 decomposition agrees with previous work: the nitro-nitrite isomerization has the lowest average energy barrier, the C–NH<sub>2</sub> bond cleavage is unlikely under the given excitation conditions, and HONO formation on the ground state surface is energy accessible but not the main process. © 2014 AIP Publishing LLC. [<http://dx.doi.org/10.1063/1.4865266>]

## I. INTRODUCTION

Development of new energetic materials with high energy storage capacity and low sensitivity with respect to temperature increase, shock, and friction events has been an active research pursuit for many years.<sup>1–3</sup> The energetic material FOX-7 (1,1-diamino-2,2-dinitroethylene,  $C_2H_4N_4O_4$ ), therefore, has recently attracted considerable attention: the synthetic process for FOX-7 has in fact been scaled up to pilot plant level in a number of countries.<sup>4–8</sup>

FOX-7 is described as a push-pull ethylene with two donor amine groups (–NH<sub>2</sub>) and two withdrawing nitro groups (–NO<sub>2</sub>) on the molecular (ethylene) framework: its insensitivity behavior can be explained by its structure.<sup>1,9–11</sup> FOX-7 is stable partially due to the strong intra-molecular hydrogen bonds between nitro oxygen atoms and amino hydrogen atoms,<sup>4,12,13</sup> which are important for its ground and excited electronic state properties. The FOX-7 crystal appears golden yellow and has two-dimensional wave-shaped layers with extensive intermolecular hydrogen bonding within the layers and with weaker van der Waals interactions between the layers.<sup>14,15</sup> Stresses in the crystal are reduced by the relative movement of layers, and in this manner, the crystal is not sensitive to mechanical strain.<sup>5</sup> Compared to the presently most widely used and powerful explosives RDX and HMX, FOX-7 yields the same number of moles (0.0405) of gaseous product per gram of compound for the complete decomposi-

tion reaction to CO<sub>2</sub>, N<sub>2</sub>, and H<sub>2</sub>O: this is, of course, the key determination of explosive and propellant performance.<sup>1,3,16</sup>

The synthesis and its mechanism, molecular structure, thermal behavior, explosive performance, and applications of FOX-7 have all been previously explored. The C–NO<sub>2</sub> bond is the most sensitive one under external loading and the C–NO<sub>2</sub> cleavage can trigger the decomposition of FOX-7.<sup>1,4,7,17,18</sup> The highest occupied molecular orbital (HOMO) and the lowest unoccupied molecular orbital (LUMO) are mostly related to the p functions for both oxygen and nitrogen atoms from the NO<sub>2</sub> groups and p functions of the carbon atom attached to the NO<sub>2</sub> group.<sup>19</sup> The typical trend for a nitro group containing energetic is that the greater the bond dissociation energy for the R–NO<sub>2</sub> bond, the lower the sensitivity is.<sup>3</sup> The ground electronic state gas phase FOX-7 dissociation energy has been studied theoretically by Politzer *et al.*, who find that the calculated C–NO<sub>2</sub> dissociation energy of FOX-7 is 70 kcal/mol, which is much lower than its C–NH<sub>2</sub> dissociation energy.<sup>11</sup> Gindulyte *et al.* proposed that the first step of FOX-7 decomposition is the NO<sub>2</sub> group transformation to –O–N–O (a nitro-nitrite isomerization), which costs 59.7 kcal/mol: for direct C–NO<sub>2</sub> bond dissociation, the energy barrier is 73 kcal/mol.<sup>16,19</sup> Kimmel *et al.* find that the C–NO<sub>2</sub> bond fission reaction requires 67 kcal/mol energy and the energy barrier for C–ONO isomer transformation is 64 kcal/mol.<sup>17</sup> C=C and C–NH<sub>2</sub> bond-fission reactions do not occur in the early stages of FOX-7 decomposition because of their high energetic barriers.<sup>11,17</sup> Condensed phase FOX-7 decomposition has been studied by Kuklja *et al.* theoretically: they find C–NO<sub>2</sub> bond-breaking energy for FOX-7 in a perfect

<sup>a)</sup> Author to whom correspondence should be addressed. Electronic mail: [erb@lamar.colostate.edu](mailto:erb@lamar.colostate.edu)

crystal is 92 kcal/mol, but the presence of reversed-orientation defects lowers this value to 59 kcal/mol.<sup>18,20</sup> In sum, the theoretical nitro-nitrite isomerization energy barrier for isolated molecule FOX-7 is from 59 to 64 kcal/mol and the calculated C–NO<sub>2</sub> dissociation energy is from 67 to 73 kcal/mol. The nitro-nitrite transformation is most likely the initial decomposition step for FOX-7 and the theoretical energy barriers are almost consistent between research groups.

The experimental activation energy of solid FOX-7 in the temperature range 210–250 °C is 58 kcal/mol.<sup>4,18–20</sup> Gas phase FOX-7 decomposition has been studied by Civis *et al.* through laser-induced (193 nm) breakdown spectroscopy and selected ion flow tube mass spectrometry. In their study, a ground state dissociation mechanism for FOX-7 is proposed in which a nitro-nitrite rearrangement is the initial step followed by the secondary reactions forming NO, HONO, C<sub>2</sub>H<sub>2</sub>, etc.<sup>21</sup> Although a big difference between solid and gas phase FOX-7 exists,<sup>17</sup> the experimental study agrees with the theoretical calculations on the ground state surface.

Ground state FOX-7 dissociation has been well studied both theoretically and experimentally; however, the decomposition of FOX-7 following electronic excitation has not been specifically addressed. Electronic excitation of condensed phase energetic species has been suggested and recognized as a major factor in the release of stored energy from energetic molecules over the past 50 years.<sup>22–33</sup>

In this work, we focus on understanding the first-step in the unimolecular decomposition mechanisms for the energetic material FOX-7, following electronic excitation. Experimentally, energy resolved ns spectroscopy is employed to explore the dynamics of the reaction through elucidating the rotational and vibrational temperatures of the initial decomposition product NO. Quantum chemistry calculations (Gaussian 09, CASSCF) are utilized to generate potential energy surfaces for the ground electronic state and a number of excited electronic states. Detailed potential decomposition mechanisms for FOX-7 are determined and discussed. Through comparisons among current widely used explosives and energetic materials we have previously studied, we arrive at a better understanding of the low sensitivity property of the energetic material FOX-7.

Conical intersections between different potential energy surfaces play a key role in the ultrafast (~100 fs) decomposition mechanisms for FOX-7 initiated from excited electronic states.<sup>26,27,34</sup> Nonadiabatic unimolecular excited state chemistry is contingent upon conical intersections between two electronic states or two potential energy surfaces, and is widely employed to explain and understand the excited state chemistry of organic and inorganic molecules. These concepts and mechanisms successfully explain the experimental observations found for electronically excited FOX-7.

## II. EXPERIMENTAL PROCEDURES

The experimental setup consists of a matrix-assisted laser desorption (MALD) system, a supersonic jet expansion nozzle, and a time of flight mass spectrometer. Details of the instrumental design are described in our previous papers.<sup>35,36</sup> The nozzle used for the molecular beam generation is con-

structed from a Jordan Co. pulsed valve and a laser ablation attachment. The laser desorption head is attached to the front of the pulsed valve with three significant parts: (1) a 2 × 60 mm channel for the expansion gas from the nozzle, (2) a conical channel (3 mm at the outside and 1 mm at the intersection with gas expansion channel) for the ablation laser beam perpendicular to the expansion gas channel, and (3) a 40 mm diameter hole for the sample drum. The sample drum fits into the 40 mm hole and is simultaneously rotated and translated by a motor and gear system in the vacuum in order to present a fresh sample region to the ablation laser for each pulse. The nonvolatile samples are desorbed from the drum by 532 nm ablation laser, entrained in the flow of He carried gas under a pressure of 80 psi through the 2 × 60 mm channel in the laser desorption head and expanded into the vacuum chamber. With 80 psi He backing pressure for the closed pulsed valve, the chamber pressure remains 2 × 10<sup>-7</sup> torr; with the valve open at 10 Hz, the chamber pressure increases to 4 × 10<sup>-7</sup> torr.

The sample drum for MALD is prepared by wrapping a piece of porous filter paper around a clean Al drum. FOX-7 is a strongly dipolar molecule due to the presence of strong donating NH<sub>2</sub> and withdrawing NO<sub>2</sub> groups in the molecular framework and it is only slightly soluble in common organic solvents and water but readily dissolves in dipolar aprotic solvents.<sup>5</sup> Acetonitrile is chosen as the solvent for FOX-7 because of its high polarity (polarity index 5.8)<sup>37</sup> and low boiling point (82 °C).<sup>38</sup> The solubility of FOX-7 in acetonitrile is smaller than 0.01 mol/l at room temperature. A solution of 0.02 mol/l matrix (R6G) and FOX-7 saturated solution in acetonitrile are uniformly sprayed on the drum surface while it is rotating under a halogen heat lamp in a fume hood to make sure the sample coating is dry. An air atomizing spray nozzle (Spraying System Co.) with siphon pressure of 10 psi is used to deposit sample plus matrix on the filter paper surface. The dried drum with well-distributed sample is then placed in the laser ablation head assembly and put into the vacuum chamber for decomposition reaction studies. The FOX-7 sample is supplied by Dr. Joseph D. Mannion.

In addition to ablation laser, one or two others laser are required to photoexcite the sample in the beam and then detect the photodissociated fragments. For NO detection, a single pump/probe laser is used at 226/236/248 nm for both initiation of the energetic molecule decomposition and detection of the NO product following a one color (1 + 1) resonance-enhanced two photon ionization (R2PI) scheme [A(v' = 0) ← X(v'' = 0–2) and I ← A transitions] through TOFMS. The proper UV laser wavelengths for this process are generated by a dye laser, pumped by the second harmonic (532 nm) of a Nd: yttrium aluminum garnet laser's fundamental output (1.064 μm), in conjunction with a wavelength extension system. The typical pulse energy of the UV laser is 50–700 μJ/pulse, which gives an intensity of ~ (2.0 × 10<sup>7</sup>)–(2.8 × 10<sup>8</sup>) W/cm<sup>2</sup> for a 8 ns pulse duration. The molecular beam is perpendicularly crossed by the UV laser beam, which is focused to a spot size of about 0.2 mm diameter at the ionization region of the TOFMS.

The timing sequence of pulsed nozzle, ablation laser, and excitation/ionization laser are controlled by time delay

generators (SRS DG535). The experiment is run at a repetition rate of 10 Hz. Ion signals in the TOFMS are detected by a microchannel plate (MCP) and signals are recorded and processed on a personal computer (PC) using an ADC card (Analog Devices RTI-800) and a boxcar averager (SRS SR 250).

### III. COMPUTATIONAL METHODS

All calculations are executed at the CASSCF(12,8)/6-31G(d) level of theory with the Gaussian 09 program. No symmetry restrictions are applied for the calculations. Equilibrium geometry calculations are conducted taking the total charge as neutral and the spin multiplicity as 1. To explore the excited state potential energy surfaces, the active space comprises 12 electrons distributed in 8 orbitals, denoted as CASSCF(12,8). Orbitals used for FOX-7 active space are three NO  $\sigma$  nonbonding orbitals  $n\sigma_{\text{NO}(1)}$ ,  $n\sigma_{\text{NO}(2)}$ , and  $n\sigma_{\text{NO}(3)}$ , two  $\pi$ -nonbonding orbitals  $\pi_{\text{NO}2(1)}$  and  $\pi_{\text{NO}2(2)}$ , one  $\sigma$  nonbonding orbital around the whole molecule  $n\sigma$ , one delocalized ONO  $\pi$ -antibonding orbital  $\pi_{\text{ONO}}^*$ , and one  $\pi$ -antibonding orbital of the whole molecule  $\pi^*$  as shown in Figure 1. We tried the Gaussian calculations in larger active spaces such as (14,9), (12,11), (12,10): the values for potential energy surfaces are similar to those found for the (12,8) calculation. To avoid convergence failure problems, a reduced (6,5) active space is also used initially for the excited state calculations: the CASSCF(12,8) is applied to get a more accurate potential energy. Excitation energies are calculated by state averaging over the ground and excited states with equal weights for each state. Expanded basis set is also explored and as reported previously, did not significantly changing the values.<sup>39</sup>

Critical points (minima and transition state structures) are characterized by analytical frequency calculations, and

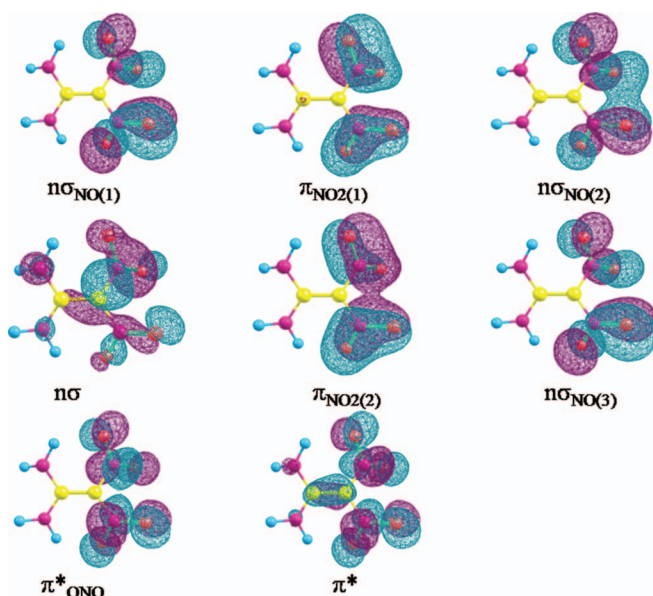


FIG. 1. Orbitals used in the active space for CASSCF calculations for FOX-7. The (12,8) active space comprises nonbonding, bonding, and antibonding  $\pi$  orbitals.

minimum energy paths are calculated using an intrinsic reaction coordinate (IRC) algorithm implemented in the Gaussian 09. FOX-7 contains two symmetric  $\text{NO}_2$  groups and to make the calculation converge, a CASSCF(6,5) is employed initially with chosen  $\text{NO}_2$  orbitals located only on one  $\text{NO}_2$  group. Following this, the (12,8) active space is applied to get a better potential energy surface. To find the transition states and intermediate states along the reaction pathways, a relaxed scan optimization algorithm as implemented is employed in which all geometrical parameters except for the specified bond distance are optimized and electronic energies are monitored as the specified bond is elongated. In the scan, the structure with peak potential energy is most likely a transition state, and the structure with potential energy in a valley is most likely an intermediate state. To verify this conclusion and obtain a more accurate potential energy surface for the transition/intermediate states, the molecular structure provided in the scan is used as the initial structure in the following optimization calculation with CASSCF(12,8) as the active space. The accuracies of the calculations along the reaction pathway are difficult to estimate since experimental information about the conical intersections and the transition states are not available. Calculations presented in this paper, however, are based on the experimental observations including decomposition products and the internal energy distributions within these products. Therefore, the proposed reaction pathways based on the computational results provide a reasonable and, at minimum qualitative, interpretation for the experimental observations.

### IV. EXPERIMENTAL RESULTS AND DISCUSSION

NO product is observed as a major decomposition product from electronically excited FOX-7 at 226/236/248 nm by TOFMS. The 226/236/248 nm excitation wavelengths also correspond to the resonance (0-0)/(0-1)/(0-2) vibronic bands of the  $\text{A}^2\Sigma^+ \leftarrow \text{X}^2\Pi$  electronic transition of the NO product. Therefore, by scanning these laser excitation wavelengths, a (1 + 1) R2PI rotationally resolved spectrum of the NO product from FOX-7 obtains. The line width of the NO mass peak is 10 ns (the laser pulse width), consistent with that expected for decomposition from the lowest few excited states. If FOX-7 were to absorb two or more photons sequentially, the NO mass signal would broaden as we have reported earlier.<sup>40</sup> Thus, the NO product is detected with two single photon absorptions for its identification, dynamics, and ionization. In this experiment, laser beam intensity is varied without change in the NO TOFMS line width, so that multiphoton dissociation of FOX-7 is unlikely. Excited electronic states of FOX-7, which might be generated in the ablation process, are effectively relaxed and cooled in the highly collisional expansion process, through the supersonic nozzle.

Figure 2 shows the spectra of three different  $\text{A}(v' = 0) \leftarrow \text{X}(v'' = 0,1,2)$  rovibronic transitions of the NO molecule generated from FOX-7. All spectra have similar rotational patterns but a varying vibrational intensity for each vibronic band. The most intense feature in each spectrum of NO corresponds to the ( $\text{Q}_{11} + \text{P}_{12}$ ) band and the lower intensity features for each vibronic transition correspond to other

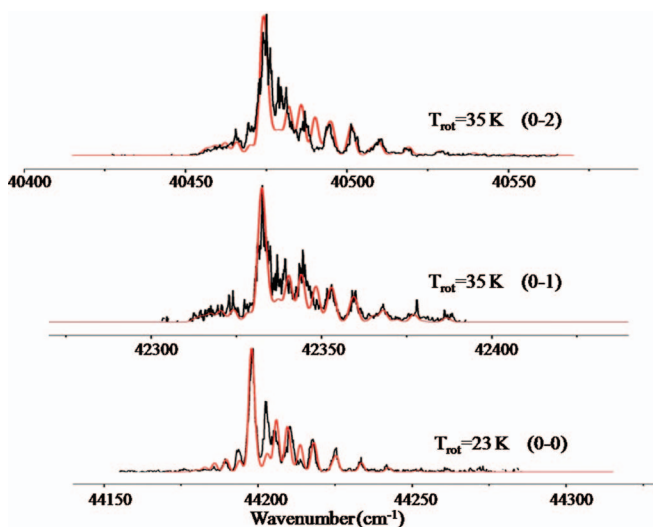


FIG. 2. One color (1 + 1) R2PI spectra of the vibronic transitions  $A^2\Sigma^+(v' = 0) \leftarrow X^2\Pi(v'' = 0,1,2)$  of the NO product from decomposition of FOX-7 following electronic excitation. Rotational simulations with a Boltzmann population distribution show that the rotation temperatures of the three observed vibrational levels on the ground electronic state (0-0), (0-1), and (0-2) are 23 K, 35 K, and 35 K, respectively, with  $\pm 10$  K uncertainty. The black line is the experimental data and the red one is the theoretical simulation for NO (A-X) transition.

rotational transitions.<sup>41</sup> Spectral simulations based on Boltzmann population distributions for the three vibronic transitions of the NO product from FOX-7 produce similar rotational temperatures ( $\sim 23$ – $35$  K) for the three vibrational levels ( $v'' = 0,1,2$ ) in the ground electronic state of NO. The vibrational temperature of the NO product can be obtained by simulating the relative intensities among the observed vibronic bands, using a Boltzmann population distribution analysis and the Frank-Condon factors. The vibrational temperature of the NO product from FOX-7 is calculated to be 2800 K, implying that FOX-7 decomposes in low lying electronic excited states. In summary, the NO product from electronically excited FOX-7 has a low rotational temperature and a high vibrational temperature, which is similar to our previous results for all NO<sub>2</sub> containing energetic molecules.

Even though the MALD technique is known to desorb easily fragile molecules in the gas phase without fragmentation, NO product is proven to be created in the excitation region in our previous studies.<sup>35</sup> The NO product can be generated from several possible mechanisms, including N–O bond breaking after nitro-nitrite isomerization, NO<sub>2</sub> photolysis, and HONO elimination. In our previous study of NO<sub>2</sub> photolysis, the rotational temperature of NO product from expansion cooled NO<sub>2</sub> gas is about 130 K for the  $A(v' = 0) \leftarrow X(v'' = 0)$  vibronic transition and the temperature goes up to 400 K for vibronic transition  $A(v' = 0) \leftarrow X(v'' = 1)$ . As the rotational temperature of the NO product from FOX-7 is much lower than that for NO<sub>2</sub> photolysis, NO<sub>2</sub> is not the precursor for NO product, and NO<sub>2</sub> loss is not the major reaction channel for the decomposition of electronically excited FOX-7.<sup>35,42–44</sup> HONO is also one of the possible intermediates in the formation of NO from FOX-7. HONO elimination for previously studied X-NO<sub>2</sub> system is less than 5% of the total NO elimi-

nation following the nitro-nitrite isomerization; moreover, the rotational temperature of NO product from HONO photolysis is extremely high.<sup>35,42</sup> Based on our ground state calculations for FOX-7 decomposition, HONO can be formed while one of the NO<sub>2</sub> groups is fragmenting from the rest of the FOX-7 molecule because of the strong intra-molecular hydrogen bond; however, as the experimental NO product has cold rotational temperatures, HONO should not be a major product. Thus, neither the NO<sub>2</sub> loss channel nor the HONO channel is present as a competitor to the nitro-nitrite isomerization/NO elimination channel. Details of the HONO channel on the ground electronic state will be discussed in Sec. V.

## V. THEORETICAL RESULTS AND DISCUSSION

The experimental results yield that the NO molecule is an initial nanosecond UV decomposition product for both electronically excited energetic and model systems. In order to understand the experimental data more completely, theoretical calculations of molecular geometries and energies for the Franck-Condon structure, conical intersections, transition states, intermediate states, and nitro-nitrite isomerizations along the ground and excited state potential energy surfaces, are performed for the energetic system FOX-7.

Two possible decomposition mechanisms are explored in the theoretical study. The first mechanism includes an excited state decomposition through transition states and a nitro-nitrite isomerization on the first excited electronic state  $S_1$  potential energy surface. The second mechanism is a ground state decomposition process that goes through a conical intersection ( $(S_1/S_0)_{CI}$ ) between the  $S_1$  and  $S_0$  states followed by an  $S_0$  nitro-nitrite isomerization. These two channels are chosen for comparison because the decomposition of energetic material FOX-7 generates NO product with a high vibrational temperature, and thus the electronic state from which dissociation occurs should have a high degree of vibrational excitation (i.e.,  $S_1$  or  $S_0$ ). The specific pathway will depend on different factors, for example, the rate of internal vibrational energy redistribution, the heights of reaction barriers, and the rate of nonadiabatic transition through the different conical intersections, and thereby the details of the low lying potential energy surfaces for FOX-7 become important.

Calculations at the CASSCF(12,8)/6-31G(d) theoretical level are employed to determine the vertical excitation energies for FOX-7 from the ground electronic state  $S_0$  to the first excited  $S_1$  and second excited  $S_2$  states. The vertical excitation energies for FOX-7 are very close to the energy of single photon excitations in the range from 226 nm to 248 nm (5.0 eV to 5.5 eV), which have been used to excite these molecules. Since there is no experimental data for vertical excitation energies of FOX-7 published so far, the experimental UV-Vis absorption spectra of FOX-7 is taken to determine the accuracy of the CASSCF calculations. The vertical excitations calculated through CASSCF(12,8)/6-31G(d) for the two lowest lying excited electronic states ( $S_1$  and  $S_2$ ) of FOX-7 are 3.49 eV and 4.27 eV, respectively. The UV-VIS absorption of FOX-7 has two maximum at 3.50 eV and 4.50 eV.<sup>45</sup> This comparison reveals that the CASSCF(12,8) method

TABLE I. Energy barriers for ground electronic state FOX-7 decomposition for nitro-nitrite isomerization, NO<sub>2</sub> formation, and NH<sub>2</sub> formation in our calculation and previous studies

	Our calculation (kcal/mol)		Previous study (kcal/mol)			
	MP2	CASSCF	B3LYP <sup>a</sup>	B3P86 <sup>b</sup>	B3LYP <sup>c</sup>	B3P86 <sup>c</sup>
TS of nitro-nitrite	60	72	63.5	...	59.1	59.7
NO <sub>2</sub> formation	76	78	66.98	70	73	73
NH <sub>2</sub> formation	112	103	110.8	111.6	...	...

<sup>a</sup>Reference 17.<sup>b</sup>Reference 11.<sup>c</sup>Reference 16.

gives a reasonable treatment of the relevant excited states: the calculated values fall into the commonly acceptable uncertainty range of  $<\pm 0.2$  eV. The CASSCF calculations show that the three lowest-lying excited states ( $S_1$ – $S_3$ ) for FOX-7 are ( $n, \pi^*$ ) transitions from the  $\sigma$  nonbonding orbital  $n\sigma_{\text{NO}}$  of NO<sub>2</sub> to delocalized ONO  $\pi$ -antibonding orbital  $\pi^*_{\text{ONO}}$  of NO<sub>2</sub> ( $S_1$  and  $S_2$ ) or  $\pi$ -antibonding orbital around the whole molecule  $\pi^*$  ( $S_3$ ). These transitions are similar to those found for the dinitroimidazole and dinitropyrazole. The potential energy surface for the  $S_3$  state of FOX-7 is above the laser excitation maximum. Thus, the  $S_3$  state is not considered in the potential energy surface calculations. From our previous studies, enlarging the basis set does not significantly improve the relative excitation energies of critical points, and therefore, a 6-31G(d) basis set is used for all calculations to maintain optimum conditions for computational cost, accuracy, and comparisons.

### A. Calculations for ground state (FC) FOX-7 decomposition

FOX-7 is famous for its low sensitivity and high performance, and thus to make a comparison with recently widely used explosives, ground state FOX-7 dissociation is studied based on its equilibrium (FC) structure. The CASSCF/6-31G(d) calculation is applied and compared with previous studies which mainly used density function theory (DFT) with hybrid B3LYP function or B3P86 function and 6-31+G(d,p) as basis set.<sup>11,16,17</sup>

Table I summarizes our CASSCF and MP2 calculation and previous theoretical work for ground state FOX-7 decomposition including the energy barriers for NO<sub>2</sub> and NH<sub>2</sub> formation and C–ONO nitro-nitrite isomerization. As shown in Table I, the bond dissociation energy of C–NH<sub>2</sub> is around 103–112 kcal/mol which is about 30 kcal/mol higher than C–NO<sub>2</sub> bond dissociation and only 3–14 kcal/mol lower than the laser energy in the present experiments; therefore the C–NH<sub>2</sub> bond is not very easy to break for the present our experimental conditions. The MP2 calculation is consistent with previous DFT studies for all three kinds of energetic barriers; however, the CASSCF calculation presents a higher transition state energy for the nitro-nitrite isomerization. The transition energy for C–ONO from the CASSCF calculation is 72 kcal/mol, 12 kcal/mol higher than the MP2 and DFT studies ( $\sim 60$  kcal/mol). The transition energy barrier for the nitro-nitrite isomerization for the CASSCF calculation decreases to 50 kcal/mol after the CASPT2 correction. Since all methods

have a ca.  $\pm 0.5$  eV acceptable error in such calculations, one can consider all of them to be reasonable. Nonetheless, we favor the CASSCF result as higher level and more physically reasonable for reaction potential energy surface calculations, because the interactions that a CASSCF algorithm considers are the essence of the potential energy surface critical points and mechanisms.

Ground state calculation shows that the most favorable reaction path for FOX-7 dissociation is nitro-nitrite isomerization/NO elimination. Another possible product from FOX-7 dissociation is the HONO molecule. HONO can be formed in the FOX-7 system because of an intra-molecular hydrogen bond between NH and ONO. Figures 3(a)–3(c) show our potential energy scans related to HONO formation. In Figure 3(a), the x-axis is the distance between the H on the NH<sub>2</sub> group and O on the nearby NO<sub>2</sub> group while the y-axis is the potential energy for each point obtained from the scan. As the distance between H and O atoms gets smaller, molecule changes from the ground state Frank Condon structure to form a HONO group while N is still bonded to C: the energy barrier is just 22 kcal/mol in this process. The HONO group is formed and still attached to the C atom with a C=C bond. The atomic distance between N on the HONO group and the C atom is scanned and the result is shown in Figure 3(b). The x-axis is the distance between the N and C atoms and the y-axis is the potential energy for each point obtained from the scan. In Figure 3(b), at small distances, the potential energy drops sharply and the FOX-7 Frank-Condon structure reforms because the FOX-7 ground state Frank Condon structure is more stable than the HONO one. As the distance between N and C increases, the NO<sub>2</sub> group moves further from the molecular system and the potential energy increases: the highest potential energy value in the scan is 80 kcal/mol at a C–N distance of 2.62 Å. A steep energy decrease (18 kcal/mol) then occurs as the distance continues to increase during this process and one H moves from the nearby NH<sub>2</sub> group to the NO<sub>2</sub> leaving group and HONO is created. Details of this process are shown in Figure 3(c): as HONO is produced, the potential energy becomes stable as HONO moves further. The energy barrier during HONO formation is modest and because of the intra-molecular hydrogen bond, hydrogen can bond to the NO<sub>2</sub> group as well as re-attach to the NH<sub>2</sub> group. Based on the experimental results, while this is possible theoretically, HONO is not the main product in the FOX-7 decomposition.

The energetic performance and sensitivity properties of FOX-7 and current widely used high performance energetic

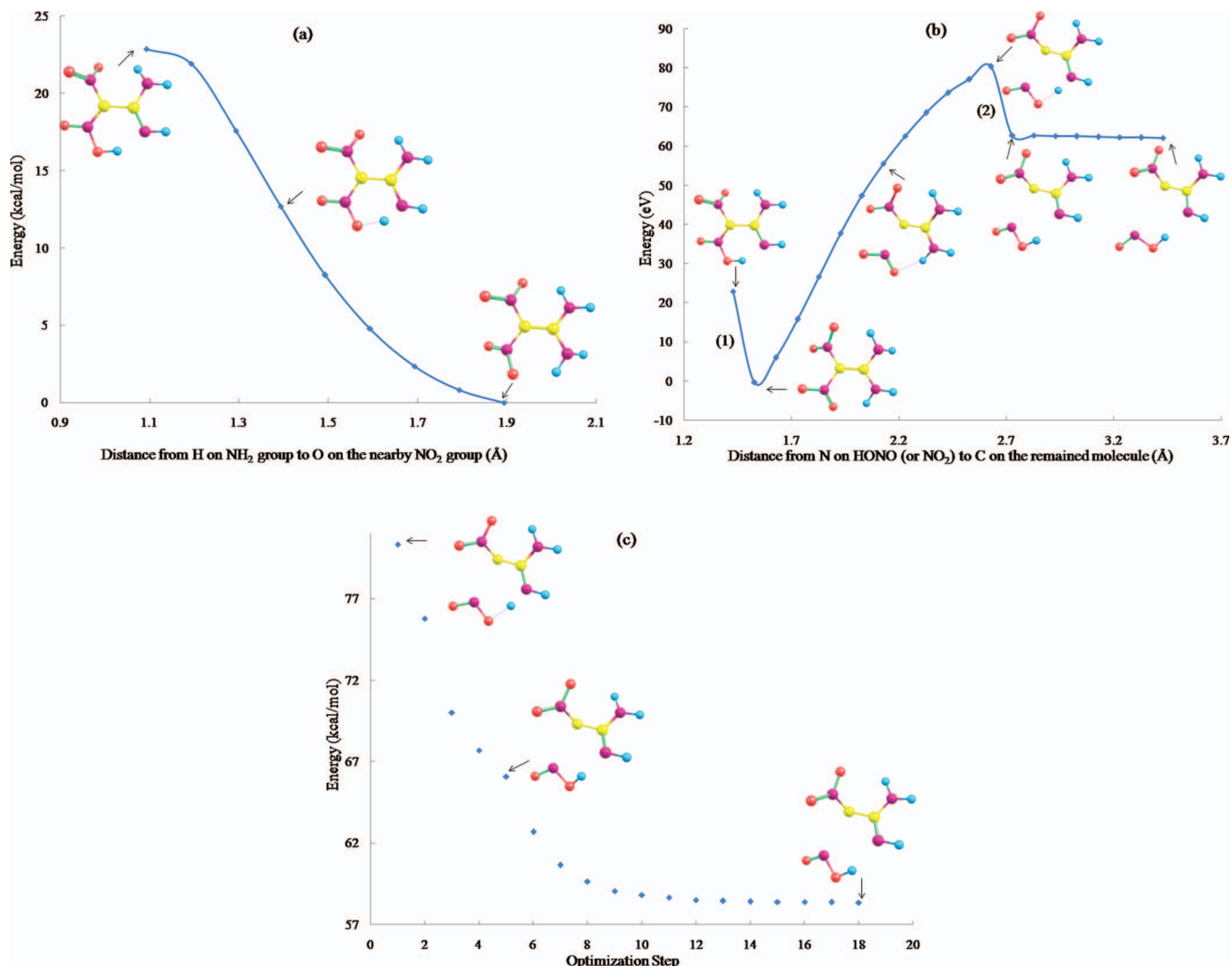


FIG. 3. (a) A relaxed scan optimization algorithm plot is presented in which all geometrical parameters except for the distance between the H on the NH<sub>2</sub> group and O on the nearby NO<sub>2</sub> group are optimized. Electronic energies are monitored as the specified bond is decreased. Molecular structures at the beginning, middle, and end of the scan are shown in the figure and arrows point out the spots related to the structures shown in the figure. The potential energy increases by 22.9 kcal/mol as HONO group (attached to C on C=C double bond) forms from the FOX-7 Frank-Condon structure. (b) A relaxed scan optimization algorithm plot is presented in which all geometrical parameters except for the distance between the N on the HONO group and the C atom of the C=C double bond is increased. Electronic energies are monitored as the specified bond is decreased. Molecular structures at the beginning, middle, and end of the scan are shown in the figure. The first energy drop which is labeled (1) in Figure 3(b) is caused by the H atom of the HONO group moving to the nearby NH<sub>2</sub> group and forming the FOX-7 Frank-Condon structure. The second energy drop which is labeled (2) in Figure 3(b) is caused by the H atom of the NH<sub>2</sub> group moving to the leaving NO<sub>2</sub> group and forming the HONO molecule. Details of this process are shown in Figure 3(c). (c) Details of the second energy drop labeled (2) in Figure 3(b). The x-axis is the number of optimization steps for the scan algorithm as C–N distance changes from 2.6 to 2.7 Å, not real reaction coordinates. During this process, H initially on the NH<sub>2</sub> group moves to the NO<sub>2</sub> group forming HONO in the system. Molecular structures at the beginning, middle, and end of the scan are shown in the figure and arrows point out the spots related to the structures shown in the figure.

materials RDX, HMX, and PETN are shown in Table II. As shown in Table II, the impact sensitivity and friction sensitivity of FOX-7 are 4–10 times higher than the other molecules, which means FOX-7 is an energetic material with low sensitivity. For energetic materials with NO<sub>2</sub> groups, the initial decomposition step from the equilibrium position on the ground state surface is usually the disruption of R–NO<sub>2</sub> bond, either through a transition state forming C–ONO nitro-nitrite isomerization or producing NO<sub>2</sub>. For RDX, HMX, and PETN, the energy barriers to NO<sub>2</sub> formation are lower than to C–ONO isomerization by about 35 kcal/mol. For the energetic material FOX-7, the energy barrier for the C–ONO transition state is lower than the NO<sub>2</sub> formation channel by about

10–20 kcal/mol. The energy barrier of FOX-7 initial decomposition step is about 20 kcal/mol higher than those for RDX, HMX, and PETN, which supports that FOX-7 is a relatively stable energetic material with low sensitivity.

## B. Calculations for electronically excited FOX-7 decomposition

A schematic one-dimensional projection of the multidimensional singlet potential energy surfaces ( $S_0$ ,  $S_1$ , and  $S_2$ ) of FOX-7, with locations and potential energies (the presented energies are not corrected for zero point energy) for different critical points and conical intersections along the minimum

TABLE II. Initial step decomposition energy barriers (nitro-nitrite isomerization and NO<sub>2</sub> formation), impact sensitivity, and friction sensitivity comparisons of currently widely used explosives RDX, HMX, PETN, and new energetic material FOX-7.

	RDX	HMX	PETN	FOX-7
TS of nitro-nitrite (kcal/mol)	92 <sup>a</sup>	46 <sup>b</sup>	60 <sup>c</sup>	72
NO <sub>2</sub> formation (kcal/mol)	41 <sup>a</sup>	38 <sup>b</sup>	35 <sup>c</sup>	78
Impact sensitivity (J)	7.5 <sup>d</sup>	7 <sup>d</sup>	3 <sup>d</sup>	>30 <sup>e</sup>
Friction sensitivity (N)	120 <sup>d</sup>	112 <sup>d</sup>	60 <sup>d</sup>	>350 <sup>e</sup>

<sup>a</sup>Reference 39.

<sup>b</sup>Reference 47.

<sup>c</sup>Reference 43.

<sup>d</sup>Reference 46.

<sup>e</sup>Reference 45.

energy reaction path, is plotted in Figure 4. The reaction coordinates depicted in Figure 4 include C–N bond lengths, ONC bond angles, and ONCC dihedral angles of the active site of FOX-7. Arrows in Figure 4 indicate different possible channels for FOX-7 decomposition. The structures of each critical point and conical intersection are summarized in Figure 5 and arrows near the transition states and conical intersections show the imaginary frequencies. In Figures 4 and 5, Frank-Condon geometry  $S_{0,FC}$  is the optimized structure of FOX-7 with minimum potential energy on the  $S_0$  state.  $(S_1/S_0)_{CI}$  is the conical intersection between the  $S_0$  and  $S_1$  states and  $(S_2/S_1)_{CI}$  is the conical intersection between the  $S_2$  and  $S_1$  states.  $S_{1,TS1}$  and  $S_{1,TS2}$  are the excited transition states on the  $S_1$  surface while  $S_{0,nitrite}$  and  $S_{1,nitrite}$  are the nitro-nitrite isomerization states on the  $S_0$  and  $S_1$  states, respectively.  $S_{0,NO}$  is the NO dissociated product on the ground state. Figure 4

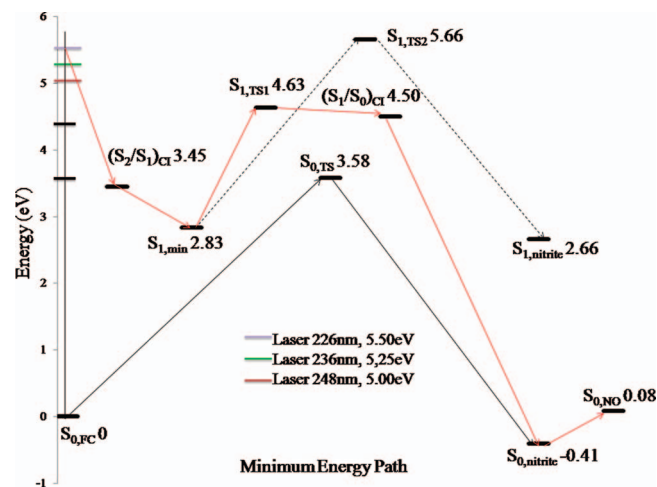


FIG. 4. A schematic one-dimensional projection of the multi-dimensional energy surfaces for FOX-7 dissociation computed at the CASSCF(12,8)/6-31G(d) level of theory. The dashed arrows represent the reaction path for NO dissociation occurring on the excited electronic state  $S_1$ : this pathway is not available based on energy considerations. The red arrows represent the reaction path on which NO is formed on the ground electronic state  $S_0$  surface: this pathway is energetically allowed. FC geometry  $S_{0,FC}$  is the optimized minimum energy structure of FOX-7 on  $S_0$  state.  $(S_1/S_0)_{CI}$  is the conical intersection between  $S_0$  and  $S_1$  states and  $(S_2/S_1)_{CI}$  is the conical intersection between  $S_2$  and  $S_1$  states.  $S_{1,TS1}$  and  $S_{1,TS2}$  are the excited transition states on the  $S_1$  surface and  $S_{0,TS}$  is the transition state on the  $S_0$  surface.  $S_{0,nitrite}$  and  $S_{1,nitrite}$  are the nitro-nitrite isomerization intermediates on the  $S_0$  and  $S_1$  states, respectively, and  $S_{0,NO}$  is the NO dissociated product on the  $S_0$  state.

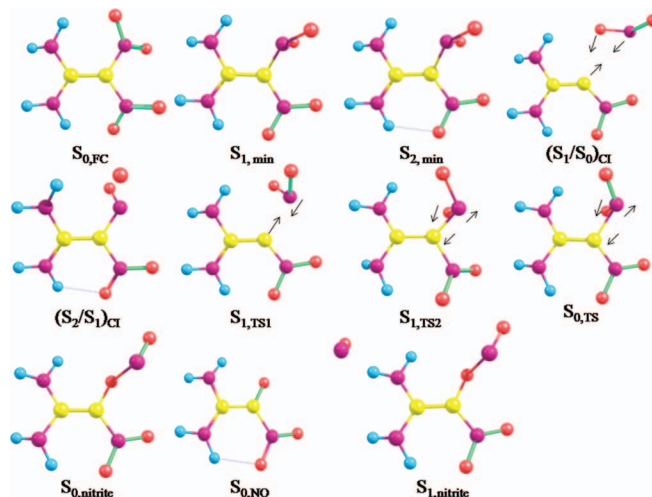


FIG. 5. Structures of all the critical points and conical intersections mentioned in Figure 4 along the FOX-7 dissociation reaction path are presented. Arrows in the structures of the transition states show the reaction coordinate associated with the imaginary frequency.

shows that following excitation to the second excited electronic state  $S_2$ , FOX-7 undergoes a rapid internal conversion from the  $S_2$  state to the  $S_1$  state through the  $(S_2/S_1)_{CI}$  conical intersection: molecules undergoing this process could in principle store sufficient vibrational energy on the  $S_1$  state, transferred from the  $S_2$  electronic energy, to dissociate. In this nonadiabatic radiationless internal conversion through  $(S_2/S_1)_{CI}$ , no significant change occurs in the nuclear configuration of FOX-7 (only some rotation of the NO<sub>2</sub> group) and no barrier exists. The adiabatic energy gap between the  $S_1$  and  $S_2$  surfaces near  $(S_1/S_2)_{CI}$  is computed to be 38 cm<sup>-1</sup> which means the  $S_1$  and  $S_2$  surfaces are strongly nonadiabatically coupled with one another and the small energy gap increases the probability of nonadiabatic transition from upper to lower electronic state. As molecules move from  $S_2$  to  $S_1$  through  $(S_2/S_1)_{CI}$ , as shown in Figure 4, FOX-7 can either decompose on the  $S_1$  excited electronic state or on the  $S_0$  ground state. If FOX-7 dissociates on the  $S_1$  state, along its nitro-nitrite isomerization path, molecules must surmount the energy barrier for the transition state  $S_{1,TS2}$  at energy 5.66 eV.  $S_{1,TS2}$  is a tight transition state, the negative frequency or unstable normal mode of which is characterized by out of plane bending of the ONCC moiety (a nitro-nitrite isomerization). But, the energy of transition state  $S_{1,TS2}$  is higher than the excitation energy limit of 5.5 eV, and therefore, FOX-7 does not have enough energy to surmount the transition state  $S_{1,TS2}$  threshold to produce NO on the  $S_1$  potential energy surface. In this case, only the nonadiabatic relaxation pathway through  $(S_1/S_0)_{CI}$  with  $S_0$  decomposition is open for FOX-7. Instead of decomposing on the  $S_1$  state, FOX-7 surmounts the energy barrier of  $S_{1,TS1}$  (4.63 eV), undergoes another nonadiabatic internal conversion to the  $S_0$  state through  $(S_1/S_0)_{CI}$  (the energy difference between  $S_1$  and  $S_0$  state is 11 cm<sup>-1</sup>) and decomposes on the  $S_0$  state via  $S_{0,nitrite}$  isomerization. The energy barrier of  $S_{1,TS1}$  is less than the energy limit for all three laser wavelengths, therefore this reaction path is energy accessible and the molecule can rapidly come back to the ground state transferring electronic excitation energy to its vibrational degrees

of freedom. The molecule isomerizes to the nitrite form on this part of its  $S_0$  surface and undergoes NO elimination, surmounting a small energy barrier ( $\sim 0.49$  eV) to the nitro-nitrite isomerization transition state. The structure near  $(S_1/S_0)_{CI}$  is a loose nitro-nitrite transition state geometry for which an  $NO_2$  moiety at the related active site of FOX-7 interacts with the rest of the molecule from a long distance ( $\sim 3.2$  Å) and this  $NO_2$  group has an out of plane  $NO_2$  bending mode with respect to the C- $NO_2$  plane. The IRC algorithm follows the bending mode of the C- $NO_2$  moiety, which ensures that conical intersection  $(S_1/S_0)_{CI}$  leads to the nitro-nitrite isomerization. A relaxed scan optimization algorithm from  $(S_1/S_0)_{CI}$  to ground state Franck-Condon structure  $S_{0,FC}$  as implemented is employed in which all geometrical parameters except for the C- $NO_2$  bond distance are optimized: electronic energies are monitored as the specified bond is decreased. The potential energy surface from the scan  $(S_1/S_0)_{CI}$  to  $S_{0,FC}$  provides a smooth potential surface without any energy peak or valley. The scan from  $(S_1/S_0)_{CI}$  to  $S_{0,nitrite}$  also proceeds without barriers or intermediates and is the steepest descents pathway for the excited molecule. As NO moves away from the rest of FOX-7 molecule along this coordinate, no obvious torque is generated on the NO product. Therefore, the NO product should have a cold rotational temperature, as is consistent with the experimental results. In sum, FOX-7 can only decompose on its  $S_0$  ground state under the current excitation conditions, generating cold rotational and hot vibrational temperatures for the NO initial product.

In the NO dissociation process, as the NO group recedes from the rest of the FOX-7 molecule, the system energy increases and becomes stable for the NO group at a distance of 3.5 Å. During the molecular decomposition on the  $S_0$  state, most of the energy stored in the molecule is transferred to the vibrational and translational energy of the NO product. This energy transfer to the nuclear coordinates enables the NO product to have a relatively high vibrational temperature. The rotational excitation of the NO product depends on the structure and reaction coordinates of the final transition state for the decomposing parent molecule. The vibrational excitation of NO depends on the stored vibrational energy in the particular electronic state in which the decomposition occurs (e.g.,  $S_0$  or  $S_1$  in this instance).

The general result is the following: all  $NO_2$  containing, excited electronic state energetic materials decompose to generate NO as the initial product from  $S_0$  with a high degree of vibrational excitation. The vibrational temperature of the initial dissociation product is important in recognizing energetic molecules because initial decomposition products with high vibrational excitation are able to propagate a chain reaction, following the initial stimulus, which leads to detonation. FOX-7 descends to the ground state through a series of conical intersections and dissociates on the ground state surface after nitro-nitrite isomerization to produce an NO initial decomposition product. Note that this chemistry occurs far from the ground state equilibrium position. Thus, conical intersections in the reaction coordinate generate products of high vibrational excitation and place the reacting molecule on a new part of its potential energy surface(s) for often very different and unanticipated new chemistry.

The FOX-7 theoretical results support that the decomposition dynamics are purely nonadiabatic in nature and that conical intersections can lead rapidly and efficiently to internal conversion from upper to lower electronic state through radiationless transition. During the internal conversion, electronic energy in the upper state is converted to vibrational energy in the lower state with a potential time scale of a few tens of femtoseconds. Conical intersections are now firmly established to be the key features in the excited electronic state chemistry of polyatomic molecules.

From our previous studies of energetic systems, the NO product from energetic materials usually has cold rotational and hot vibrational temperatures: FOX-7 behavior is consistent with that of previously studied energetic materials.<sup>34–36,40,42–44,47</sup> The difference is that for the ground state decomposition of other energetic materials with higher sensitivity,  $NO_2$  formation is more favorable than C- $NO_2$  isomerization from the Frank-Condon  $S_0$  equilibrium studies, because of a lower energetic barrier: this situation is reversed for FOX-7. Another recently studied low sensitive energetic material, 3,4-dinitropyrazole (DNP), has a similar behavior for  $NO_2$  formation vs. C- $ONO$  isomerization on the ground electronic state. The energy barriers for  $NO_2$  formation and C- $ONO$  isomerization of DNP using the MP2 algorithm are 70 kcal/mol and 58 kcal/mol, respectively, which is quite close to the FOX-7 MP2 calculated values, shown in Table I. This might be because for both FOX-7 and DNP their first few electronic excited states are of a similar orbital excitation description involving  $n\pi^*$  transitions on local  $NO_2$  groups. DNP is stabilized by the  $\pi$  orbitals on its aromatic ring and two  $NO_2$  groups, while FOX-7 is stabilized by its intra-molecular hydrogen bonding between  $NH_2$  and  $NO_2$  groups.

## VI. CONCLUSIONS

Decomposition of the energetic material FOX-7 following electronic excitation has been explored via nanosecond, energy resolved spectroscopy. NO is an initial decomposition product at the nanosecond excitation energies (5.0–5.5 eV) with vibrationally hot (2800 K) and rotationally cold ( $< 35$  K) temperatures. Based on the experimental observations and CASSCF theoretical calculations, we conclude that for the energetic material FOX-7, decomposition occurs on the  $S_0$  state potential energy surface, as  $S_1$  state decomposition is energetically unavailable. Molecules excited to the  $S_2$  state descend to the  $S_1$  and  $S_0$  states through  $(S_2/S_1)_{CI}$  and  $(S_1/S_0)_{CI}$  conical intersections, and NO is generated following a nitro-nitrite isomerization on the  $S_0$  surface. Conical intersections are the key point for the theoretical mechanisms, as they provide nonadiabatic radiationless internal conversion between upper and lower electronic states on the fs time scale. The ground state FOX-7 decomposition result is consistent with previous studies; nitro-nitrite isomerization is the most favorable reaction path, while  $NH_2$  formation is not favorable under the present excitation conditions. An HONO product is energetically accessible but not a main product in FOX-7. Compared to currently widely used energetic materials like RDX, HMX, and PETN, the ground state initial

decomposition step of FOX-7 has higher energy barriers which is part of the reason for its low sensitivity.

## ACKNOWLEDGMENTS

This study is supported by a grant from the U.S. Army Research Office (ARO, FA9550-10-1-0454) and in part by the U.S. National Science Foundation (NSF) through the XSEDE supercomputer resources provided by NCSA under Grant No. TG-CHE110083. We also want to thank Dr. Joseph D. Mannion, NSWC, Indian Head Division for supplying the FOX-7 sample used in this study.

- <sup>1</sup>X.-H. Ju, H.-M. Xiao, and Q.-Y. Xia, *J. Chem. Phys.* **119**, 10247 (2003).
- <sup>2</sup>C. Ye and J. M. Shreeve, *J. Chem. Eng. Data* **53**, 520 (2008).
- <sup>3</sup>L. Turker and S. Varis, *Z. Anorg. Allg. Chem.* **639**, 982 (2013).
- <sup>4</sup>J. Zhao and H. Liu, *Comput. Mater. Sci.* **42**, 698 (2008).
- <sup>5</sup>J. Anniyappan, M. B. Talawar, G. M. Gore, S. Venugopalan, and B. R. Gandhe, *Journal of Hazardous Materials* **137**, 812 (2006).
- <sup>6</sup>M. M. Kuklja, F. J. Zerilli, and S. M. Peiris, *J. Chem. Phys.* **118**, 11073 (2003).
- <sup>7</sup>Q. Wu, W. Zhu, and H. Xiao, *J. Mol. Model.* **19**, 4039 (2013).
- <sup>8</sup>A. Hu, B. Larade, H. Abou-Rachid, and L.-S. Lussier, *Propellants, Explos., Pyrotech.* **31**, 355 (2006).
- <sup>9</sup>M. M. Bishop, R. S. Chellappa, M. Pravica, J. Coe, Z. Liu, D. Dattlebaum, Y. Vohra, and N. Velisavljevic, *J. Chem. Phys.* **137**, 174304 (2012).
- <sup>10</sup>K. Xu, J. Song, F. Zhao, H. Ma, H. Gao, C. Chang, Y. Ren, and R. Hu, *J. Hazard. Mater.* **158**, 333 (2008).
- <sup>11</sup>P. Politzer, M. C. Concha, M. E. Grice, J. S. Murray, P. Lane, and D. Habibollahzadeh, *J. Mol. Struct.* **452**, 75 (1998).
- <sup>12</sup>M.-H. Liu, K.-F. Cheng, C. Chen, and Y.-S. Hong, *Int. J. Quantum Chem.* **110**, 813 (2010).
- <sup>13</sup>C. J. Wu, L. H. Yang, L. E. Fried, J. Quenneville, and T. J. Martinez, *Phys. Rev. B: Condens. Matter* **67**, 235101 (2003).
- <sup>14</sup>M. Pravica, Y. Liu, J. Robinson, N. Velisavljevic, Z. Liu, and M. Galley, *J. Appl. Phys.* **111**, 103534 (2012).
- <sup>15</sup>W. P. C. de Klerk, C. Popescu, and A. E. D. M. van der Heijden, *J. Therm. Anal. Calorim.* **72**, 955 (2003).
- <sup>16</sup>A. Gindulyte, L. Massa, L. Huang, and J. Larle, *J. Chem. Phys. A* **103**, 11045 (1999).
- <sup>17</sup>A. V. Kimmel, P. V. Sushko, A. L. Shluger, and M. M. Kuklja, *J. Chem. Phys.* **126**, 234711 (2007).
- <sup>18</sup>M. M. Kuklja, S. N. Rashkeev, and F. J. Zerilli, *AIP Conf. Proc.* **845**, 535 (2006).
- <sup>19</sup>S. N. Rashkeev, M. M. Kuklja, and F. J. Zerilli, *Appl. Phys. Lett.* **82**, 1371 (2003).
- <sup>20</sup>M. M. Kuklja, S. N. Rashkeev, and F. J. Zerilli, *AIP Conf. Proc.* **706**, 363 (2004).
- <sup>21</sup>M. Civis, S. Civis, K. Sovova, K. Dryahina, P. Spanel, and M. Kyncl, *Anal. Chem.* **83**, 1069 (2011).
- <sup>22</sup>B. M. Rice, S. Sahu, and F. J. Owens, *J. Mol. Struct.: THEOCHEM* **583**, 69 (2002).
- <sup>23</sup>B. Tan, X. Long, R. Peng, H. Li, B. Jin, S. Chu, and H. Dong, *J. Hazard. Mater.* **183**, 908 (2010).
- <sup>24</sup>M. R. Manaa, L. E. Fried, C. F. Melius, M. Elstner, and Th. Frauenheim, *J. Phys. Chem. A* **106**, 9024 (2002).
- <sup>25</sup>A. B. Kunz, M. M. Kuklja, T. R. Botcher, and T. P. Russell, *Thermochim. Acta* **384**, 279 (2002).
- <sup>26</sup>M. M. Kuklja, *J. Appl. Phys.* **89**, 4156 (2001).
- <sup>27</sup>E. J. Reed, J. D. Joannopoulos, and L. E. Fried, *Phys. Rev. B* **62**, 16500 (2000).
- <sup>28</sup>M. R. Manaa and L. E. Fried, *J. Phys. Chem. A* **103**, 9349 (1999).
- <sup>29</sup>B. Tan, R. Peng, X. Long, H. Li, B. Jin, and S. Chu, *J. Mol. Model.* **18**, 583 (2012).
- <sup>30</sup>B. Tan, X. Long, J. Li, F. Nie, and J. Huang, *J. Mol. Model.* **18**, 5127 (2012).
- <sup>31</sup>A. B. Kunz and D. R. Beck, *Phys. Rev. B* **36**, 7580 (1987).
- <sup>32</sup>C. M. Tarver, *AIP Conf. Proc.* **1426**, 227 (2012).
- <sup>33</sup>S. H. Lee, K. C. Tang, I. C. Chen, M. Schmitt, J. P. Shaffer, T. Schultz, J. G. Underwood, M. Z. Zgierski, and A. Stolow, *J. Phys. Chem. A* **106**, 8979 (2002).
- <sup>34</sup>A. Bhattacharya, Y. Q. Guo, and E. R. Bernstein, *Acc. Chem. Res.* **43**, 1476 (2010).
- <sup>35</sup>Y. Q. Guo, A. Bhattacharya, and E. R. Bernstein, *J. Chem. Phys.* **122**, 244310 (2005).
- <sup>36</sup>Y. Q. Guo, M. Greemfield, A. Bhattacharya, and E. R. Bernstein, *J. Chem. Phys.* **127**, 154301 (2007).
- <sup>37</sup>S. Lindsay, *High Performance Liquid Chromatography*, 2nd ed. (Thames Polytechnic, London, 1992), Chap. 6, p. 120.
- <sup>38</sup>R. L. Brown and S. E. Stein, "Boiling Point Data" in NIST Chemistry WebBook, NIST Standard Reference Database Number 69, edited by P. J. Linstrom and W. G. Mallard (National Institute of Standards and Technology, Gaithersburg MD), <http://webbook.nist.gov> (2013).
- <sup>39</sup>A. Bhattacharya and E. R. Bernstein, *J. Phys. Chem. A* **115**, 4135 (2011).
- <sup>40</sup>A. Bhattacharya, Y. Q. Guo, and E. R. Bernstein, *J. Chem. Phys.* **131**, 194304 (2009).
- <sup>41</sup>C. J. S. M. Simpson, P. T. Griffiths, H. L. Wallaart, and M. Towrie, *Chem. Phys. Lett.* **263**, 19 (1996).
- <sup>42</sup>A. Bhattacharya, Y. Q. Guo, and E. R. Bernstein, *J. Phys. Chem. A* **113**, 811 (2009).
- <sup>43</sup>Z. Yu and E. R. Bernstein, *J. Chem. Phys.* **135**, 154305 (2011).
- <sup>44</sup>Z. Yu and E. R. Bernstein, *J. Chem. Phys.* **137**, 114303 (2012).
- <sup>45</sup>L. Simkova, J. Urban, J. Klima, and J. Ludvic, *Int. Rev. Chem. Eng.* **4**, 554 (2012).
- <sup>46</sup>R. Mayer, J. Kohler, and A. Homburg, *Explosives*, 5th ed. (Wiley-VCH, Weinheim, 2002).
- <sup>47</sup>O. Sharia and M. M. Kuklja, *J. Phys. Chem. A* **114**, 12656 (2010).